# Research of Fuel Characteristic of Dimethyl ether/High Viscosity & Incombustible matter Blend for Marine Diesel Engine

MIHARA, Yu ; KURO-OKA, Daiki ; SHIRAHAMA, Tomoki ; KUWAOKA, Kenta ; SUZUKI, Takashi ; ASANO, Ichiro ; DAN, Tomohisa

JSAE 20190XXX
SAE 2019-YY-YYYY

# Research of Fuel Characteristic of Dimethyl ether / High Viscosity & Incombustible matter Blend for Marine Diesel Engine

**Yu MIHARA, Daiki KURO-OKA, Tomoki SHIRAHAMA, Kenta KUWAOKA, Takashi SUZUKI, Ichiro ASANO, Tomohisa DAN**
Graduate School of Maritime Sciences, Kobe University



## ABSTRACT

Diesel engine has fuel combustion capability in various high density oil such as residual fuels or biofuels derived from fossil or living matter. But for commercial use, these fuels except bio diesel fuel (BDF) should be heated, separated and filtered by equipment and dosed or mixed with additive or distillate oil etc. before being supplied to the engine in order to improve combustibility.

This study aims to illuminate fuel characteristic of blend contained woody pyrolysis oil (WPO) which is high viscosity and incombustible, and dimethyl ether (DME) whose emission of combustion has no soot particle. This paper describes thermo-physical property of neat WPO and the blend on the basis of the evaluation of fuel fluidity by measurement and calculation of viscosity.

According to the result, it was confirmed that the fluidity of WPO was improved by mixing DME and the approximate viscosity expressions at any temperature of WPO and the blend were good accuracy.

## INTRODUCTION

Diesel engine has high efficiency and combustibility even in the case of applying heavy oil such as marine residual fuels which contain components like vacuum residue (VR), light cycle oil (LCO), clarified oil (CLO) and sludge as base, diluent and sediment materials. On the other hands, low environmental burden fuel (e.g. liquefied natural gas (LNG), low sulfur gas oil (LSGO), ultra-low-sulfur fuel (ULSF) etc.) and its optimum application method have been developed because of pollutants included in emission from conventional marine diesel engine. Furthermore, biofuels like BDF derived from plant oil with esterification is also alternative marine fuels of which $CO_2$ emission is carbon neutral[1]. In addition to BDF, the research of raw plant oil or wasted edible oil without esterification applicable to marine diesel engine as well as automotive diesel engine has been studied and it is confirmed that the combustion characteristic improves at high load operation of the engine[2].

In the actual vessel, although bunker-C oil is available to diesel engine, the pre-treatments such as heating with steam or electric power, centrifuging by separator and dosing with additives etc. are quite required in order to retain the appropriate fluidity and prevent carbon deposit associated with long term of bad combustion. In terms of this pre-treatment, it is supposed that blend fuel is a kind of dosing additive and the most practical application of unfavorable materials to vessel, which are low cost but also high viscosity and incombustible.

BFNE (Biofuels with non-esterification for simplicity) applicable to diesel engine is useful in terms of not only low environmental burden of the emission and good combustion at high load but also lower cost and shorter production process than BDF. WPO is one of BFNE and derived from woody biomass mainly wasted in forestry. Diesel engine fueled Neat WPO can run, whereas the long term running i.e. actual use is still hard owing to remarkable incombustibility[3]. On the other hands, new fuel injection system is being developed which improves combustion characteristic of BFNE at low engine load[4]. In contrast, it is supposed that the onboard pretreatment of incombustible fuel by dosing additive as shown above i.e. blend with improver of combustibility and fluidity is one of more retrofit and cost effective utilization to apply BFNE to marine diesel engine, and useful in the sense that low economic materials can convert to worthwhile one as fuel.

In the field of this research, the availability of dimethyl ether (DME) and bunker oil blend which decreases pollutants in emission of diesel engine and improves flow-ability of the oil have been confirmed[5][6]. According to this method, authors attempted to improve properties of WPO which was difficult to be utilized as fuel without some pretreatment.

## FUEL SAMPLE SPECIFICATION

### THE SPECIFICATION OF WPO

WPO sample for this research is produced as follow[7].

(1) Sawdust is compressed and converted to a briquette.
(2) The briquette is heated until 1473 K by a kiln.
(3) The solid content becomes charcoal and the gas content is cooled and liquefied then becomes WPO.

WPO is not standardized individually as product and the detail information was not offered from selling agency. Additionally, it was considered that the manufacturing process of the WPO wasn't unified strictly, and the process differed the properties of the oil every time it was produced. From the above, the WPO for this research was divided into non-distilled and distilled WPO (NWP and DWP) as light and heavy WPO to take the various qualities into consideration. Before the viscosity test, the density of test fuels at 286-323 K was measured. Fig. 1 shows the results of density measurement, and the approximate expressions.

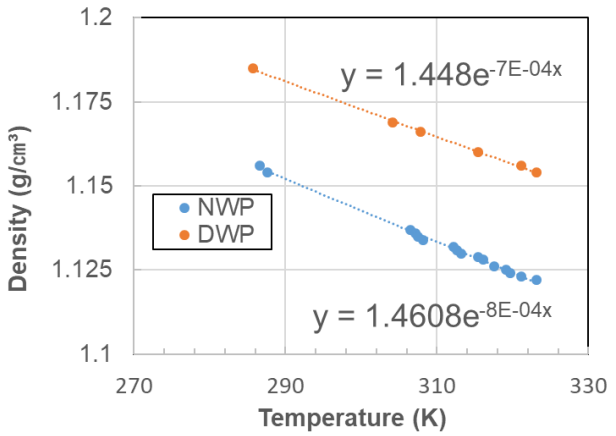


Fig. 1 WPO density and the approximate expressions based on the measurement

### THE SPECIFICATION OF DME

DME is ether of which carbon bond is mediated by oxygen therefore it includes no soot in the combustion emission. The phase is gas under atmospheric condition and becomes liquid at below 248 K of temperature and over 0.6MPa of pressure. And DME is primarily produced by dehydration of methanol in the current industrial. Table 1 showed the basic properties of DME[8], and light oil based on Japanese Industrial Standards (JIS) K 2204-2007[9] which is reference of typical fuel of diesel engine.

Table 1 Basic properties of DME and light oil

| | DME | Light oil |
|---|---|---|
| Chemical Formula | $CH_3OCH_3$ | - |
| Liquid density (g/cm$^3$, 293K) | 0.67 | - |
| Liquid density (g/cm$^3$, 288K) | - | ≦0.86 |
| Viscosity (mPa·sec, 293K) | 0.15 | - |
| Kinematic viscosity (mm$^2$/sec, 293K) | 0.22 | - |
| Kinematic viscosity (mm$^2$/sec, 303K) | - | ≧1.7 |

## EXPERIMENTAL APPALATUS AND PROCEDURE

### MEASUREMENT AND CALCULATION METHODOLOGY OF VISCOSITY

Pre-experiment

In order to narrow the test range of temperature of sample, viscosity coefficients of NWP and DWP were preliminarily measured by Brookfield viscometer which is type of rotational single cylinder (spindle). The exterior and the measurement system of the viscometer were shown in Fig. 2-3. According to Fig. 3, a temperature of heat transfer oil in a thermostatic oil bath was controlled by heating, stirring and monitoring with heating element, a stick and thermometer. Test sample in the container which was immersed in the heat transfer oil was also stirred then experimental temperature was controlled through the oil and detected at the point shown in Fig. 3 by thermocouple. Subsequently, spindle of the viscometer was set and the measurement was performed after the temperatures of the sample and the oil showed no difference between them. The measurement procedure on the basis of AMETEK Brookfield's instruction is as follow. The spindle immersed in the sample oil is rotated by electrical motor. Viscosity is indicated on the display when the revolving spindle of the meter detects rotation rate (rpm) in steady and torque (%) in normal range. Shear rate and shear stress is calculated by equation [1] and [2].

$$S = 4\pi \cdot N \cdot R_B^2 \cdot R_S^2 / 60x^2 \cdot (R_B^2 - R_S^2) \quad [1]$$

$$\tau = 0.001\eta \cdot S \quad [2]$$

Here, S, N, $R_B$, $R_S$, x, τ and η is shear rate (sec$^{-1}$), rotation rate (rpm), diameter of oil bath (cm), diameter of spindle (cm), diameter to be calculated for shear rate (cm), shear stress (Pa) and viscosity coefficient (mPa·sec) respectively. In this research, it was regarded that shear rate S was at the surface of spindle therefore $R_S$ was substituted to x of equation [1] and S was indicated anew as equation [3][10].

$$S = 4\pi \cdot N \cdot R_B^2 / 60(R_B^2 - R_S^2) \quad [3]$$


Fig. 2 Brookfield viscometer

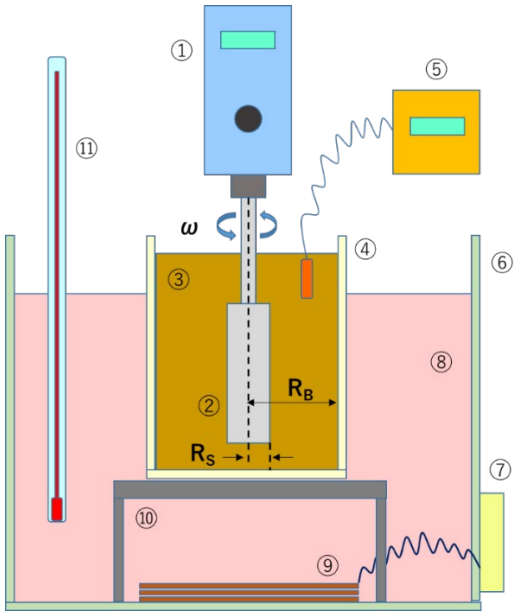


① Viscometer
② Spindle
③ Test sample
④ Sample container
⑤ Thermocouple &Temp. monitor
⑥ Thermostatic oil bath
⑦ Temp. controller
⑧ Heat transfer oil
⑨ Heating element
⑩ Container holder
⑪ Thermometer

Fig. 3 Schematic diagram of viscosity measurement by Brookfield viscometer

The viscosity (mPa·sec) and the rotation rate (rpm) of viscometer and the temperature (K) of thermostatic oil bath for test samples were measured respectively. The viscometer indicates actual value on the basis of converted value from spindle torque detected, however, available range of measurement is defined by spindle geometry and the torque is impossible to be detected if the available range is over. Therefore the measurement was performed with modification by changing type of spindle and temperature of samples.

Main experiment

Zeitfuchs Cross-Arm viscometer was applied for the measurement of kinematic viscosity of DWP and the blend with DME as main experiment. The exterior of the viscometer was shown in Fig. 4. The test range of kinematic viscosity is limited to maximum 1000 $mm^2/sec$ therefore temperature for test should be determined within approximate range. And the viscometer was kept pressurized condition by nitrogen gas and pressure cell shown in Fig. 5 so as to preserve liquid phase of DME.

Experimental apparatus and measurement system shown in Fig 6 were as follow. The outside of pressure cell was immersed into the water in thermostatic bath and test temperature of sample in the cell was maintained via air or nitrogen gas and the water. The ambience temperature in pressure cell was monitored by thermocouple and thermometer. In case of blend, nitrogen gas reservoir was connected to pressure sample tank with mixer and pressure cell with viscometer, and the gas was supplied to them ((a) and (b) in Fig. 6). Schematic diagram of pressure sample tank with mixer was shown in Fig. 7. As the figure shows, WPO sampled from the reservoir was initially poured into the tank then DME was supplied to the bottom by way of the circle pipe. Finally, the sample was pressurized by $N_2$ over corresponding saturated vapor pressure and blended by mixing propeller. Test sample was flew from the sample tank to pressure cell via supply valve, dripped and collected into viscometer ((c)). In the Fig. 4, the sample was dripped from the top of (1) broad tube and collected in (2) horizontal tube. As time progressed, liquid level of the sample reached and crossed line A then it was drawn from (3) inverted U-shape tube by capillarity. Thereafter the sample was fell via (4) straight tube and rose from (5) U-shape tube then reached (6) measuring section. Here, efflux time when sample passed between two line B and C was measured.

Generally, measurement value v ($mm^2/sec$) is obtained by multiplying viscometer constant $C_1$ ($mm^2/sec^2$) and efflux time t (sec) together as shown in equation [4].

$$v = C_1 \cdot t \qquad [4]$$

On the other hands, it was possible that the viscosity of blend sample indicated lower than actual value owing to reduction of sample efflux time t due to pressurization by nitrogen gas. Therefore in this research, viscosity v of blend sample was corrected to v' ($mm^2/sec$) by modification coefficient $C_2$ (-) shown in Table 2 and equation [5] which were devised by Ryu[6]

$$v' = C_1 \cdot C_2 \cdot t \qquad [5]$$

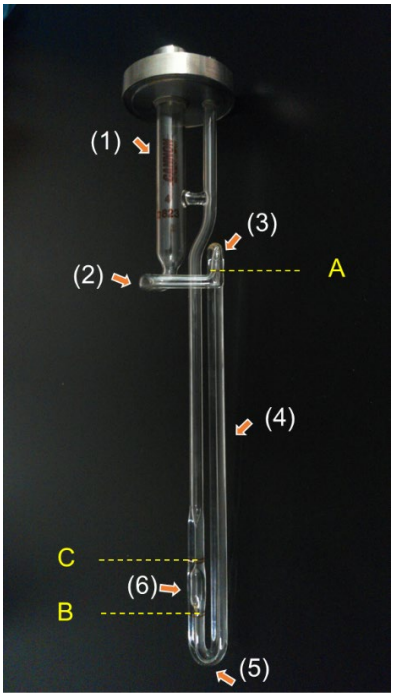


Fig.4 Zeitfuchs Cross-Arm viscometer

Fig. 5 Pressure cell to close and retain ambient space and temperature of the viscometer

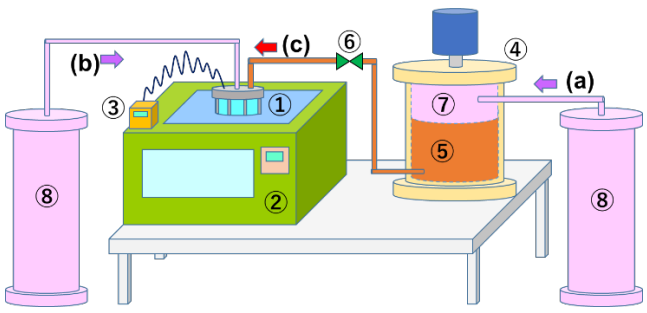


① Pressure cell with viscometer
② Thermostatic bath
③ Thermometer
④ Pressure sample tank with mixer
⑤ Sample to be measured
⑥ Supply valve to viscometer
⑦ Nitrogen gas pressurizing
⑧ Nitrogen gas reservoir

Fig. 6 Schematic diagram of viscosity measurement by Zeitfuchs Cross-Arm viscometer

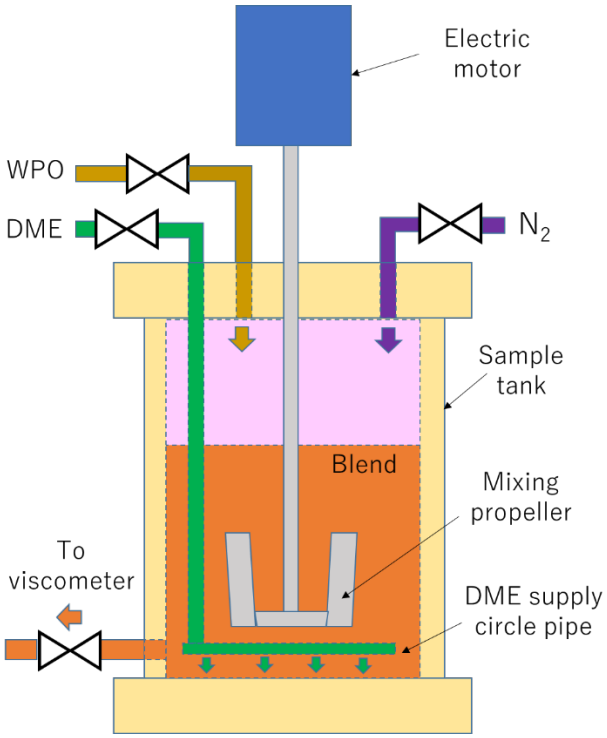


Fig. 7 Schematic makeup of pressure sample tank with mixer in Fig. 6

Table 2 Pressure coefficient for experimental kinematic viscosity

| Test pressure [MPa] | 1.0 | 1.3 | 2.0 |
|---|---|---|---|
| Coefficien $C_1$ [$mm^2/sec^2$] based on JIS K 2283-2000 | 1.0 | | |
| Coefficien $C_2$ [ - ] based on experiments | 1.25 | 1.27 | 1.34 |

## RESULTS AND DISCUSSION

PRE-EXPERIMENT

Viscosity coefficient and shear stress versus shear rate

Fig.9 and 10 showed the test result of NWP and DWP. In this experiment, the test temperature available to obtain enough number of measurement was applied therefore the result showed that the temperatures were not unified between NWP and DWP. It was because that spindle torque of viscometer indicated failure due to over range of viscosity when rotation speed (rpm) was manually changed even though sample temperature was constant. In addition, maximum and minimum point in Fig. 9 and 10 meant upper and lower limit of

experimental value at the temperature since the torque indicated failure when the speed of viscometer was increased or decreased over or under the points.

According to the results in Fig. 9 and 10, measured viscosity of both NWP and DWP increased as shear speed increased in same temperature, and decreased as temperature decreased. And the DWP viscosity had tendency to increase approximately 20 times in comparison with NWP at the temperature from 317 to 324 K.

On the other hand, although viscosities both NWP and DWP showed non-Newtonian of which viscosity increases as shear speed increases, the increase rate of viscosities decreased conversely. Therefore it was considered that the viscosities finally indicated constant. Therefore the correlation of viscosity η for shear speed S shown in Fig. 9 and 10 was approximated by convex quadratic function with variable S, which passed point 1 to 3 of actual values and showed polar ACB (exactly polar AC) in Fig. 8. It was possible to regarded that viscosity η was saturated at point C where the first derivate of S was 0 namely the slope of line DC was horizontal then η indicated no increase as line CE. Accordingly, it was supposed that shear speed S corresponding to this C at which η reached just convergence value was obtained. And the value of S was substituted to the derivate which was equal to zero then viscosities at each temperature was acquired as typical values respectively in this experiment. The values were also shown in Fig. 9 and 10 as extreme value.

Fig. 11 and 12 displayed shear stress (Pa) versus shear speed ($sec^{-1}$) and the relation indicated linear tendency. Accordingly, it was supposed that NWP and DWP conformed to Newton's law of viscosity designated by equation [2] as far as this experimental conditions.

As Fig. 13 and 14 displayed, it was clear that calculated constant viscosity of NWP and DWP increased exponentially for increment of temperature.

Although this paper does not describe, it was confirmed that the viscosity of cooled NWP after being heated had tendency to increase apparently even though the measurement temperature before and after heating were same.

In the results of pre-experiment, it was obvious that viscosity of both NWP and DWP had tendency to increase and saturate simultaneously and gradually due to possible non-Newtonian. On the other hands, actual convergence of shear speed S and viscosity η were not confirmed owing to limited maximum revolution of the viscometer. Hence the actual values of viscosity η and shear speed S were determined expediently based on approximation of the relations of η for S by quadratic function. However, it appeared that above approximation was not enough precise method in order to measure kinematic viscosity using capillary tube with proper range. Consequently, analysis of measurement value was executed again, applying another approximation to derive estimation expression for viscosity η.

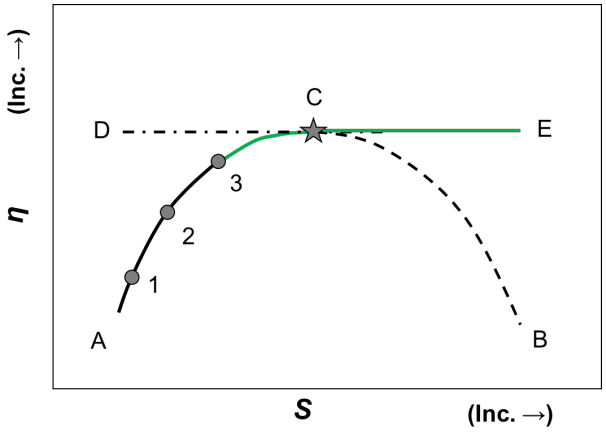


Fig. 8 Method to determine converged viscosity

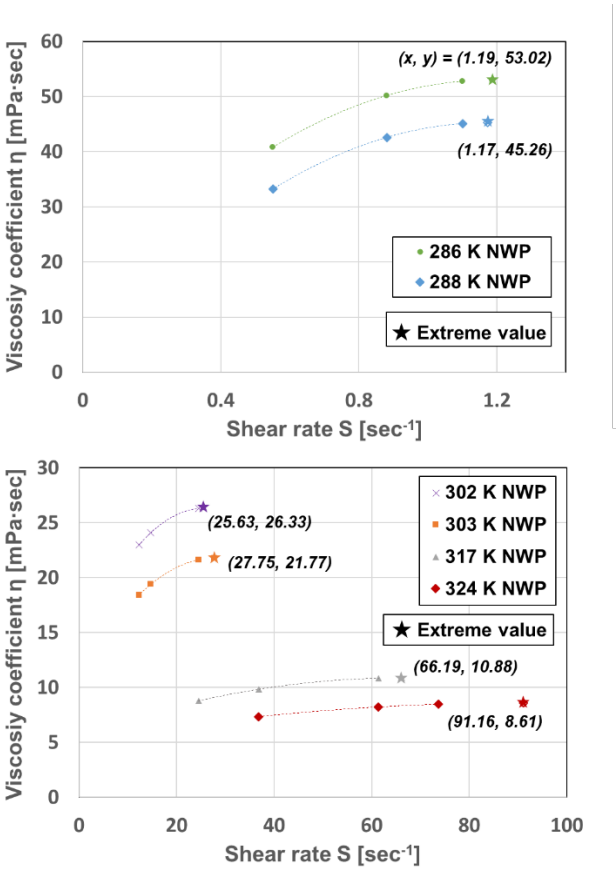


Fig. 9 Viscosity for shear rate of NWP

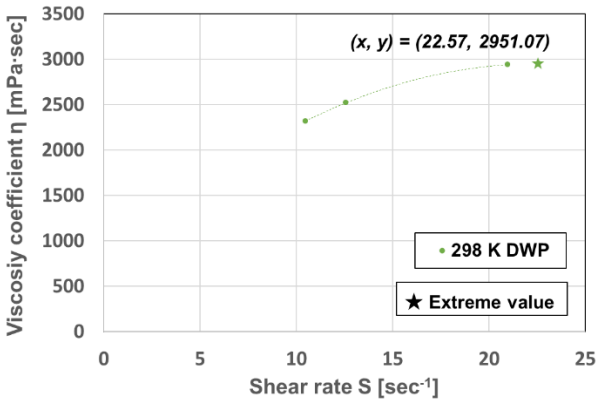


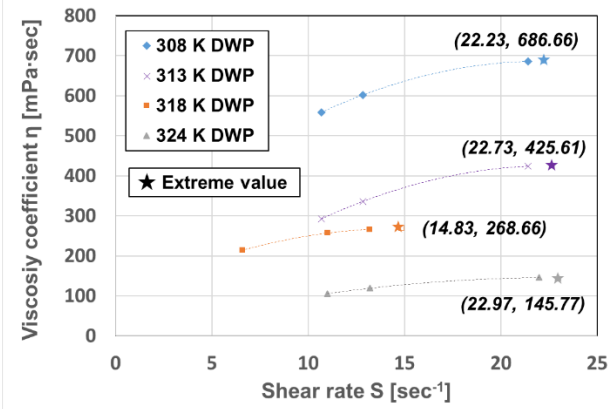


Fig. 10 Viscosity for shear rate of DWP

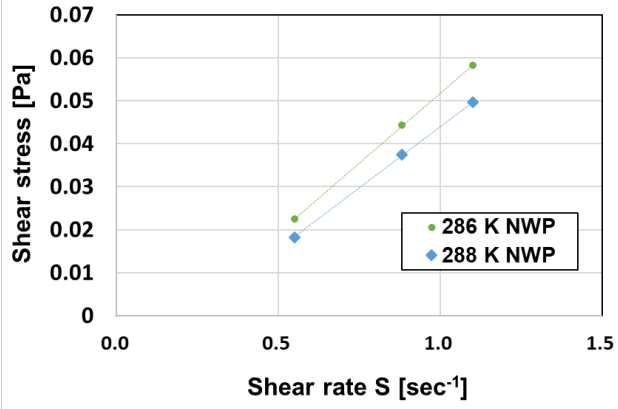


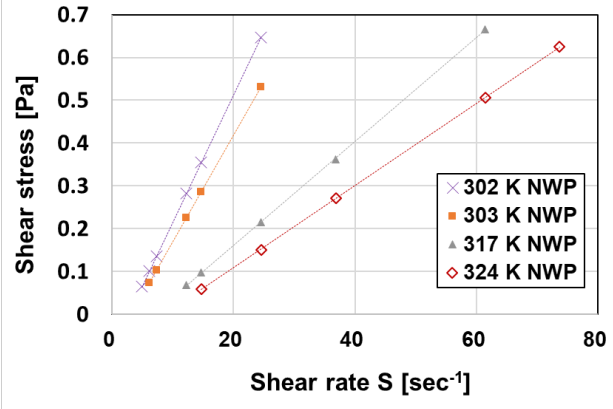


Fig. 11 Shear stress for shear rate of NWP

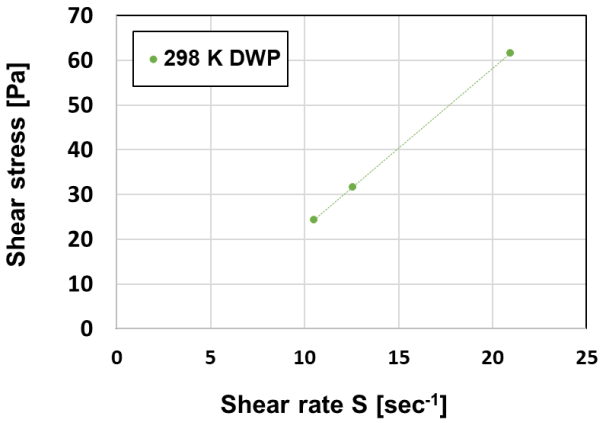


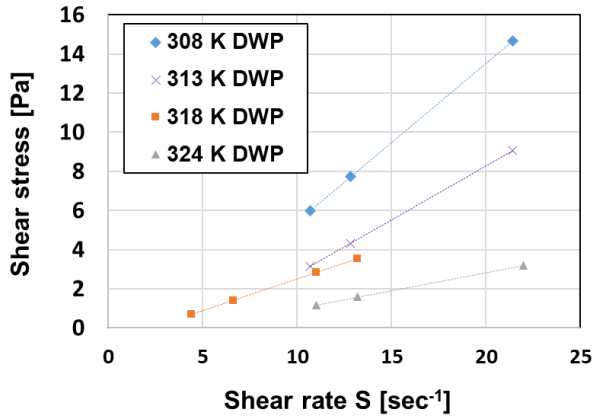


Fig. 12 Shear stress for shear rate of DWP

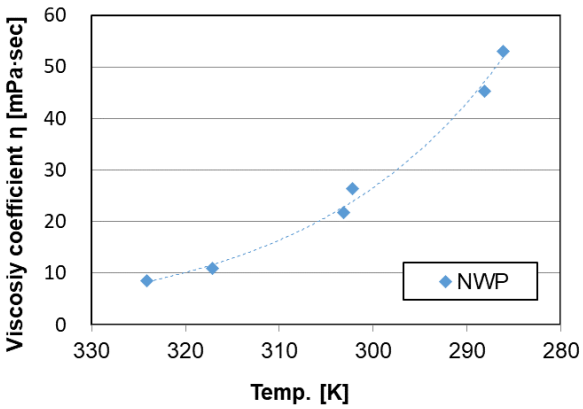


Fig. 13 Viscosity of NWP based on extreme value of quadratic function on Fig. 9

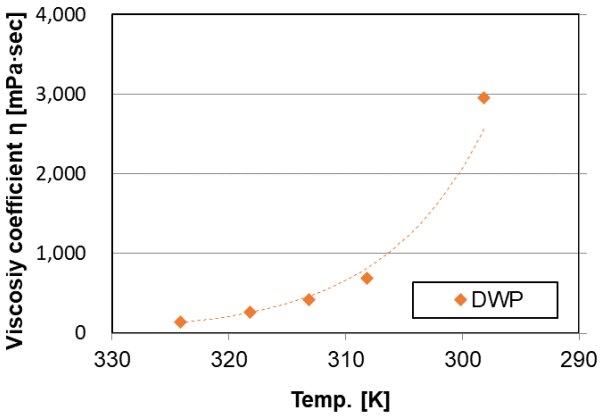


Fig. 14 Viscosity of DWP based on extreme value of quadratic function on Fig. 10

Back ground of derived expression for estimation of viscosity versus temperature

In this section, a background of derivation of expression to estimate viscosity was shown especially NWP for example. Refer next section for equations [6] – [12], Fig. 17 and Table 3 – 5 described in this section.

(1) Firstly, Andrade's formula [6] was introduced as fundamental form of expression, which is known as equation describing the relation of viscosity versus temperature of liquid.

(2) Secondly, according to the results of viscosity measurement shown in Fig. 9, exponential function which has Napier's constant and variable x as a base and an index (hereinafter called "Exp. (x)") was applied to estimate convergence value in wider range than that of approximation by convex quadratic function shown in Fig. 8. The example of estimation based on this function was shown in Fig. 17 of which right direction meant decrease of the inverse of shear rate S and also indicated increase of S. Fig. 17 showed that Exp. (x) converged at some value when x namely shear rate S (the number of revolutions of the viscometer) became infinity and that the approximate equations indicated similarity with Andrade's formula [6] of function for temperature while they were function for shear rate. Therefore it could be argued that [6] was actually applied as fundamental form.

(3) Here, Fig. 15 showed the comparison of above two approximation which were method by $\eta_{NQ}$ and by $\eta_{NE}$. The method by $\eta_{NQ}$ using quadratic function A-C-B was based on estimated value shown as point C on the figure, which converged at neighborhood of maximum measurement value 3 corresponding to maximum point (1.19, 53.02) – point (99.16, 8.61) for 286 K to 324 K in Fig. 9. On one hand, method by $\eta_{NE}$ using exponential function A-G was founded on supposed value as point G saturated at extremely far distance from value 3. In this paper, it was regarded that $\eta_{NQ}$ and $\eta_{NE}$ was lower and upper limit value respectively in the estimation range where actual convergence value of viscosity η existed. And the values of $\eta_{NQ}$ and $\eta_{NE}$ corresponding to 286 K – 324 K were calculated on the basis of above methods.

(4) Next, a standard value $\eta_m$ for 286 K – 324 K to estimate η in the range between limit $\eta_{NQ}$ and $\eta_{NE}$ was calculated as the intermediate value of the limits. Then approximate equation [7] was obtained on the basis of the relation of the standard values for temperature T, which was function of T, and was similar to Andrade's formula [6]. Table 3 showed calculated values of $\eta_{NQ}$, $\eta_{NE}$ and $\eta_m$.

(5) In addition, it was confirmed that shear rate S and coefficient M shown as the values 1.19 – 91.61 and 0.289 – 13.83 (with equations) in Fig. 9 and 17, which was related to $\eta_{NQ}$ and $\eta_{NE}$ had the relation to temperature severally as shown in equation [8], [9], Table 4 and 5.

(6) Accordingly, equation F [10] was obtained converting B and T in the formula [6] to coefficient M and shear rate S above. Comparing equation [7] and [10] which were the form equal to [6], it was reasonable to assume that S and M which reflected $\eta_{NQ}$ and $\eta_{NE}$ were connected with the standard value $\eta_m$ in the range of estimation via temperature T.

(7) As a result of variously examining about method of application of F approaching $\eta_m$ toward actual convergence value, ratio of $\eta_{NE}$ to F concerning each actual shear speed and temperature showed tendency to approximate with errors of 1-18% (Fig. 16). In the largest range of the errors of 10-18%, the errors which were converted to viscosity coefficient showed 1-3 and 1 mPa·sec for the range of measurement value of 12-24 and 5-12 mPa·sec at 303 K and 317 K. Consequently, it was supposed that $\eta_m$ was approximated to the actual value up to a point utilizing this application method of F.

(8) In consequence, calculated values of viscosity according to $\eta_R$ [11] as fundamental expression to estimate viscosity, which was the ratio of $\eta_m$ to F, was fallen under the estimation range between limit $\eta_{NQ}$ and $\eta_{NE}$.

(9) Finally, the relation of calculated values from [11] for temperature was approximated and estimation expression for NWP viscosity $\eta_N$ [12] was derived as function of temperature T.

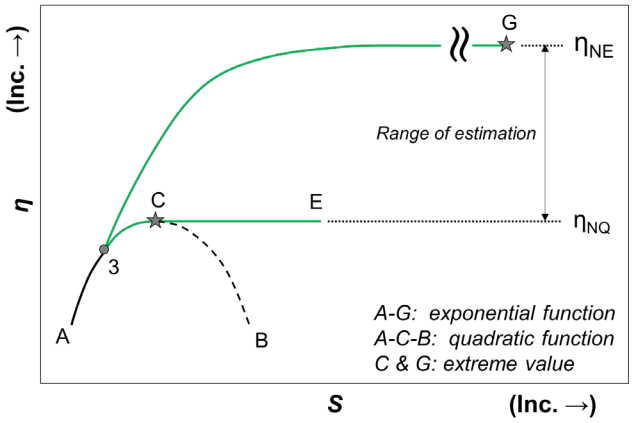


Fig. 15 Meaning of $\eta_{NQ}$ and $\eta_{NE}$

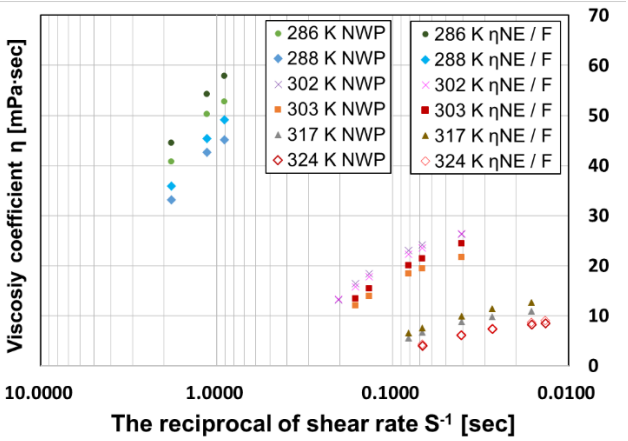


Fig. 16 The comparison of actual values and estimation by $\eta_{NE}$ for F in non-Newtonian domain

Practice of deriving the expression

In order to derive the expression to estimate viscosity of NWP and DWP at any temperature, Andrade's formula [6] was applied.

$$\eta_a = A \exp (B/T) \quad [6]$$

Here, $\eta_a$, exp, A, B and T was viscosity coefficient (mPa·sec), exponential function, base coefficient, exponent coefficient and temperature (K) respectively. For example, derivate process of the expression for NWP was shown as follow.

The correlation of viscosity η (mPa·sec) versus shear rate S ($sec^{-1}$) of NWP and the exponential approximate equations were shown in Fig. 17. According to the equations, the viscosity at each temperature were converged to constant value when the reciprocal of shear rate $S^{-1}$ progressed to neighborhood of zero i.e. shear rate S became infinity. The constant values corresponded to base coefficient of the equations in Fig. 17. Namely, it was considered that the values were equivalent to coefficient A of formula [6]. Consequently, it was assumed that actual viscosity of NWP existed between viscosity $\eta_{NQ}$ and $\eta_{NE}$ which were based on extreme value of quadratic and exponential function displayed in Fig. 9 and 17. Therefore intermediate value $\eta_m$ between $\eta_{NQ}$ and $\eta_{NE}$ (Table 3) was plotted for temperature and the approximate equation $\eta_m$ [7] was obtained.

$$\eta_m = 6.0 \cdot 10^{-6} \exp (4611.1 / T) \quad [7]$$

The expression to be derived was analogized from formula [6] and equation [7].

Next, it was supposed that the absolute value M of exponent coefficient of the equations shown in Fig. 17 had a correlation versus temperature (K) as shown in Table 4. Then approximate equation of M for temperature T (K) was obtained as follow.

$$M = 0.0044\ T^2 - 2.3503\ T + 309.17 \quad [8]$$

Furthermore, shear rate S corresponding to extreme value of viscosity displayed in Fig. 9 had also a correlation for temperature (K) as Table 4 shown then equation of S [9] was obtained.

$$S = 0.0372\ T^2 - 20.273\ T + 2759.2 \quad [9]$$

From above, exponential function F of which exponent coefficient was the ratio of M to S was considered.

$$F = \exp (M/S) \quad [10]$$

In accordance with equation [7] and [10], $\eta_R$ shown in [11] was obtained.

$$\eta_R = 6.0 \cdot 10^{-6} \exp (4611.1 / T - M/S) \quad [11]$$

Finally, using equation [11], search for the desired expression was performed considering that $\eta_R$ was actual viscosity and satisfying that the calculated value was between $\eta_{NQ}$ and $\eta_{NE}$. As a result of the search, the expression available to estimate viscosity $\eta_N$ of NWP was acquired as shown in [12]

$$\eta_N = 3.0 \cdot 10^{-6} \exp (4835.8 / T) \quad [12]$$

Correspondingly, the expression $\eta_D$ of DWP was acquired as shown in [13]

$$\eta_D = 7.0 \cdot 10^{-14} \exp (11460.0 / T) \quad [13]$$

Fig. 18 and 19 displayed kinematic viscosity estimated by Fig. 1, expression [12] and [13]. Although the expressions and figures were able to calculate kinematic viscosity of NWP and DWP at any temperature, these were deficient in practicality due to possibility of 0.5 to 2.0 times of error for actual value.

As the results in this experiment demonstrates, it was difficult to measure WPO viscosity which changed after heating even short time and increased for shear rate namely non-Newtonian indicated in the results of measurement by rotational single cylinder type. In consequence, the viscosity was only estimated in a wide range by the expressions and figures above. On the other hand, actual kinematic viscosity is uniquely determined by capillary viscometer. Additionally, it was supposed that the result by the method could give good accuracy expression to estimate the viscosity at any temperature.

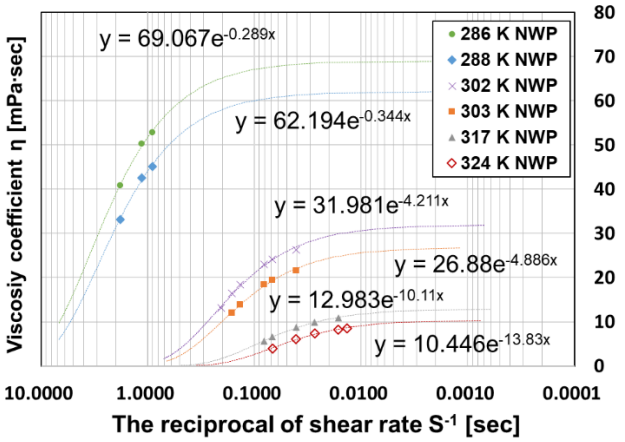


Fig. 17 Viscosity for the reciprocal of shear rate in the logarithmic scale of NWP

Table 3 Viscosity of NWP $\eta_{NQ}$, $\eta_{NE}$ and $\eta_m$ based on the extreme values in Fig. 9, 17 and the averages

| Temp. [K] | $\eta_{NQ}$ [mPa·s] | $\eta_{NE}$ [mPa·s] | $\eta_m$ [mPa·s] |
|---|---|---|---|
| 286 | 53.02 | 69.07 | 61.04 |
| 288 | 45.26 | 62.19 | 53.73 |
| 302 | 26.33 | 31.98 | 29.16 |
| 303 | 21.77 | 26.88 | 24.33 |
| 317 | 10.88 | 12.98 | 11.93 |
| 324 | 8.61 | 10.45 | 9.53 |

Table 4 Absolute value M of the exponent coefficients of the exponential functions in Fig. 17

| Temp. [K] | M |
|---|---|
| 286 | 0.29 |
| 288 | 0.34 |
| 302 | 4.21 |
| 303 | 4.89 |
| 317 | 10.11 |
| 324 | 13.83 |

Table 5 Approximate shear rate S of NWP based on the extreme values of quadratic functions in Fig. 9

| Temp. [K] | S [sec$^{-1}$] |
|---|---|
| 286 | 1.19 |
| 288 | 1.17 |
| 302 | 25.63 |
| 303 | 27.75 |
| 317 | 66.19 |
| 324 | 91.16 |

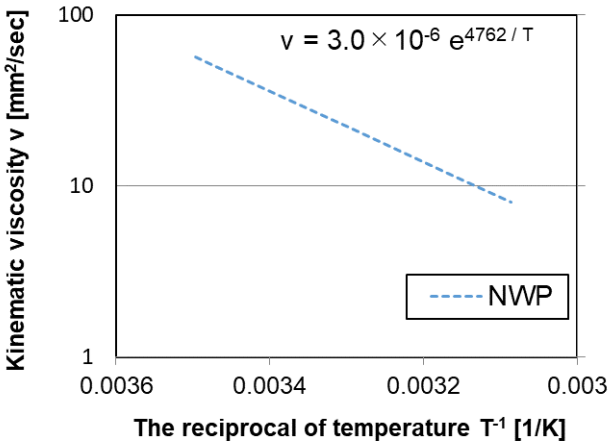


Fig. 18 Estimated kinematic viscosity of NWP based on the approximate expression [12]

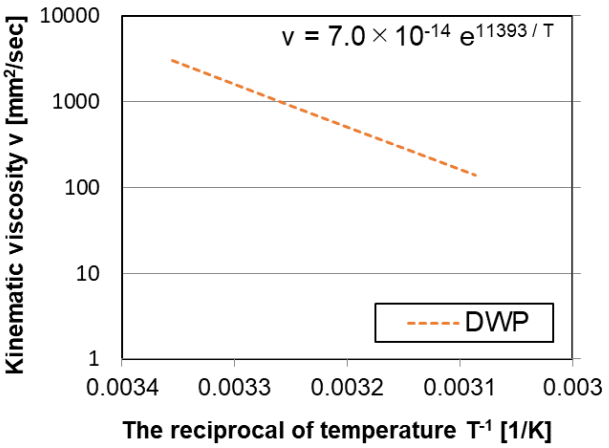


Fig. 19 Estimated kinematic viscosity of DWP based on the approximate expression [13]

MAIN EXPERIMENT

Kinematic viscosity of DWP and Blend

According to the result of pre-experiment, it was apparent that the viscosity of WPO became high due to distilling. From the perspective of improvement of high viscosity matter, kinematic viscosity of two

samples which were high viscos DWP and DWP/DME blend was measured based on capillary viscometer.

The mixing ratio of DWP / DME was set seven to three originally applied for bunker-C / DME blend fuel which has characteristic of improvement of heat efficiency and reduction of particulate matter (PM) at low engine load[(5)]. Hereafter, sample for neat of DWP, 70 wt% of DWP with 30 wt% of DME blend was abbreviated as WP100 and WP70D30 respectively.

Test temperatures were set 313, 323, 333 K according to upper limit of measurement (1000 $mm^2$/sec). Additionally, test pressures were also set 1.3 MPa for 313 and 323 K and 2.0MPa for 333 K in order to retain the liquid phase of DME at each temperature and to apply pressure coefficient for modification of the measurement value on the basis of Fig. 20 which was DME saturated vapor pressure diagram[(8)], and Table 2. And kinematic viscosity was measured three times at each test temperature for 2 samples and the average values were determined as actual values.

The test results and the approximate equations of WP100 and WP70D30 (Blend) were shown in Fig. 21 and 22. As the figures indicated, it was considered that each actual viscosity v ($mm^2$/sec) had a relation for temperature (K) as Andrade's formula [6].

Table 6 and 7 showed the comparison of experimental values and estimated values calculated by the equations in Fig.21, 22. The accuracy of the estimations for actual values of WP100 and WP70D30 represented about 1.6 % and 10-14%, and the error of the latter was large in comparison with the former. DWP used for WP70D30 was not able to reuse for subsequent experiment and was sampled newly every measurement. Therefore, it was assumed that the error was derived from scattered density of WP70D30 containing DWP collected from the supernatant or the residue in the reservoir. But it is possible to improve the accuracy owing to review and revise of the experimental procedure in future.

From the standpoint of general proper range of fuel viscosity at inlet of marine diesel engine (15 ± 5 $mm^2$/sec, recommended by the manufactures), the error of WP70D30 was within 1-3 $mm^2$/sec. Consequently, it was considered that the estimated expression of blend was available to practical use, whereas it was required that actual data of the viscosity was kept storing because of present non-standardization of WPO properties as fuel.

Finally, decrease rate of kinematic viscosity of WP70D30 for WP100 was shown in Table 8. Mixing with DME, the viscosity of DWP decreased approximately 90 %.

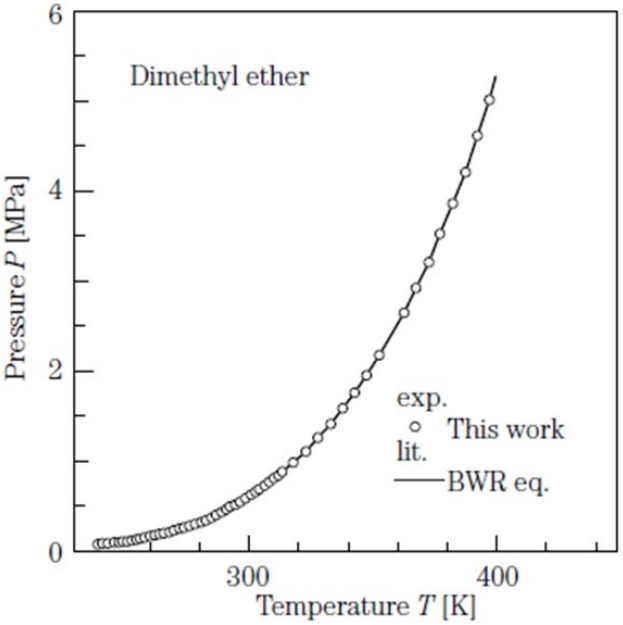


Fig. 20 Saturated vapor pressure of DME quoted from DME Handbook Edited by Japan DME forum, p46

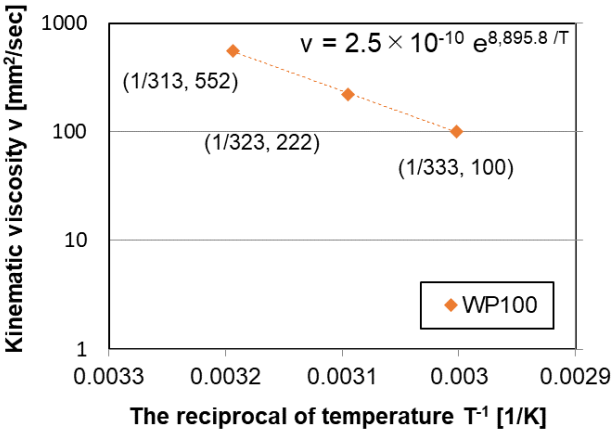


Fig. 21 Experimental kinematic viscosity of DWP for reciprocal of the temperature in a logarithmic scale

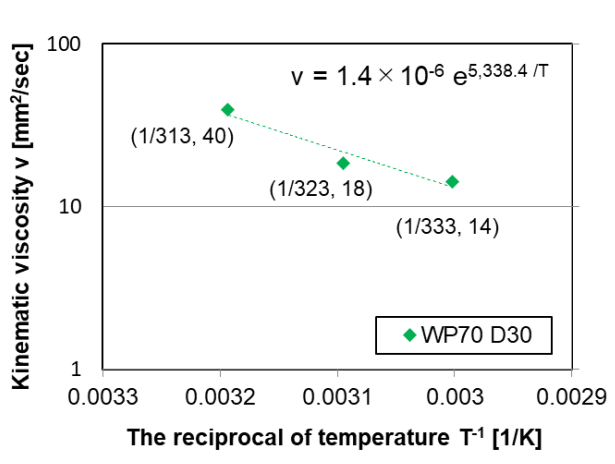


Fig. 22 Experimental kinematic viscosity of Blend for reciprocal of the temperature in a logarithmic scale

Table 6 The comparison of experimental and estimated kinematic viscosity of WP100

| Temp. [K] | Kinematic viscosity v [mm$^2$/sec] | | | Error of (1) and (3) [%] |
|---|---|---|---|---|
| | Exp. WP 100 | | (3) Est. WP 100 | |
| | (1) Average | (2) SD | | |
| 313.15 | 552.08 | 8.15 | 543.44 | 1.57 |
| 323.15 | 221.90 | 1.28 | 225.62 | 1.67 |
| 333.15 | 100.38 | 2.85 | 98.74 | 1.63 |

Table 7 The comparison of experimental and estimated kinematic viscosity of WP70D30

| Temp. [K] | Kinematic viscosity v [mm$^2$/sec] | | | Error of (1) and (3) [%] |
|---|---|---|---|---|
| | Exp. WP70D30 | | (3) Est. WP70D30 | |
| | (1) Average | (2) SD | | |
| 313.15 | 39.53 | 2.78 | 35.46 | 10.30 |
| 323.15 | 18.42 | 0.63 | 20.92 | 13.59 |
| 333.15 | 14.28 | 0.53 | 12.74 | 10.74 |

Table 8 The decrease rate of kinematic viscosity of WP100 and WP70D30

| Temp. [K] | Kinematic viscosity v [mm$^2$/sec] | | Decrease rate of (1) to (2) [%] |
|---|---|---|---|
| | (1) Exp. WP 100 | (2) Exp. WP70D30 | |
| 313.15 | 552.08 | 39.53 | 92.84 |
| 323.15 | 221.90 | 18.42 | 91.70 |
| 333.15 | 100.38 | 14.28 | 85.78 |

## EVALUATIONS OF DWP AND BLEND AS FUEL

In order to evaluate high viscos DWP and the blend with DME as fuel for diesel engine, experimental viscosity of WP100, WP70D30, bunker-C (C100) and the blend with DME, of which mixing rate was seven to three (C70D30) were plotted versus temperature for comparison (Fig. 23). In accordance with Fig. 23, it was considered that the viscosity of DWP as WP100 and WP70D30 was affected by the change of temperature remarkably in comparison with bunker-C as C100 and C70D30. And it was apparent that WP70D30 had flow characteristic almost equal to C70D30.

And Table 9 showed comparison of estimated temperatures among 4 samples by approximate equations based on Fig. 23. The temperatures corresponded to the proper range of fuel viscosity at marine diesel engine inlet recommended by the manufactures. Table 9 indicated that WP100 was required to heat until 354-364 K, whereas 324-338 K of fuel temperature satisfied with proper fluidity of WP70D30. On the other hand, desired temperature of DWP was lower than bunker-C due to higher decrease rate of viscosity versus increment of temperature.

Combustion characteristic of WPO / DME blend based on fuel vaporization, atomization and engine performance is to be investigated in future research.

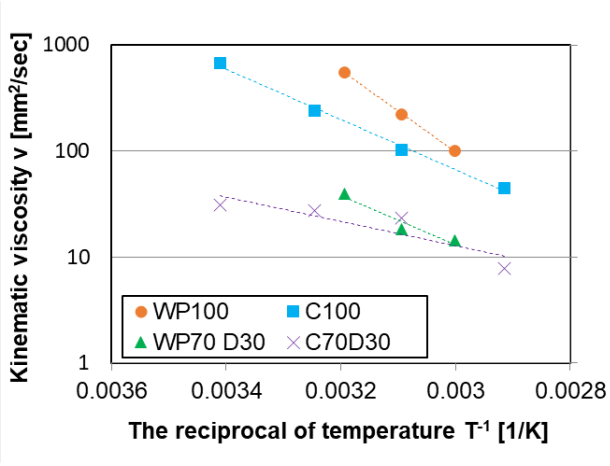


Fig. 23 Evaluation of WPO and the blend based on experimental viscosity of bunker-C and DME blend by Ryu, Y. [6]

Table 9 Estimated temperature for recommended kinematic viscosity of marine diesel engine by the engine manufactures

| Fuel samples | Kinematic viscosity [mm$^2$/sec] | |
|---|---|---|
| | 10 | 20 |
| | Fuel temperature [K] | |
| WP100 | 364 | 354 |
| WP70 D30 | 338 | 324 |
| C100 | 377 | 360 |
| C70D30 | 344 | 316 |

## CONCLUSION

In this study, thermo-physical properties of pre-treated high viscos WPO by blending with DME was examined. The summary of this research were as follow.

1. Viscosity coefficients of non-distilled and distilled WPO were measured and the results show that the latter has tendency to increase 10 to 25 times in comparison with the former at same temperature.

2. Kinematic viscosities of distilled WPO and the blend with DME were measured and the results indicate that the fluidity as the viscosity of the WPO improves about 90 % by mixing DME, and the estimated kinematic viscosity is calculated in good accuracy by derived expressions.

3. On the basis of the experimental results, distilled WPO and DME blend was evaluated as fuel and the results showed that the fluidity as the viscosity becomes approximately equal to bunker-C and DME blend of which improvement of heat efficiency and environmental burden are confirmed.

## REFERENCES


1. Nakao S., R & D for Marine Engine Using Biofuel -Application of Refined Bleached Deodorized Palm Oil (RBDPO), Journal of the JIME Vol.51, No.1, 66-71, 2016
2. Nishio S. et al., Combustion and Exhaust Characteristics of Rapeseed Oil in Marine Diesel Engine, Journal of the JIME Vol.45, No.5, 120-126, 2010
3. Yamane K. et al., Combustion and Exhaust Emission Characteristics of Diesel Engines Fueled with Wood-Derived Pyrolysis Tar Oil, Transactions of Society of Automotive Engineers of Japan Vol.35, No.1, 83-88, 2004
4. Nishio S. et al., Study on Marine Engine Control for Multi-Fuel-Study on Combustion Technology of Bio-Fuel, Construction of Combustion Control System and Proof Experiment-, Papers of National Maritime Research Institute Vol.14, No.1, 11-36, 2014
5. Yoshida K. et al., Combustion Analysis of Bunker Oil DME Mixed Fuel in Pre-Combustion Chamber Type Diesel Engine, Proc. of the 10th ISME, Harbin, 2014
6. Ryu Y. et al., Improvement of Bunker Oil by Using Liquefied Dimethyl Ether for Diesel Engine Application, Doctoral Dissertation of Kobe University, Kobe, 2013
7. Kuramoti Y., Consideration from Production of Briquette of Compressed Sawdust, and Sawdust Charcoal [Translated from Japanese.] http://www001.upp.so-net.ne.jp/ito-hi/satoyama/bn/015kuramoti.html Last access date 2018.12.14
8. Japan DME Forum, DME Hand Book Edited by Japan DME Forum, 2007
9. Japanese Industrial Standards Committee, JIS Hand Book 25 Petroleum 2016 [Translated from Japanese.], 2016
10. Onoyama M. et al., Viscosity Measurements of Petroleum Products with the Brookfield-Type Rotational Viscometer, Journal of The Japan Petroleum Institute Vol.8, No.4, 25-28, 1965